Fizika Nizkikh Temperatur, 2006, v. 32, No. 11, p. 1441–1448

The polymerization of acetylene on supported metal clusters

S. Gilb, M. Arenz, and U. Heiz

Technische Universität München, Lehrstuhl für Physikalische Chemie
Lichtenbergstr. 4, 85747 Garching, Germany
E-mail: ulrich.heiz@mytum.de

Received May 29, 2006, revised August 29, 2006

The polymerization of acetylene was studied by thermal programmed reaction on model catalysts consisting of size-selected Ag, Rh, and Pd atoms and Pd_n $(1 \le n \le 30)$ clusters on well-characterized MgO(111) thin films. In a single-pass heating cycle experiment, benzene, butadiene, and butane were catalyzed with different selectivities as function of cluster size: palladium and rhodium atoms selectively produce benzene, and the highest selectivity for butadiene is observed for Pd_6, whereas Pd_{20} reveals the highest selectivity for butane. Ag atoms are inert. These results provide an atom-by-atom observation of the selectivity of small cluster catalysts.

PACS: 82.33.Hk, **82.65.+r**, 36.40.Jn

Keywords: small clusters catalysts, cyclotrimerization reaction, Ag, Rh, and Pd atoms, dependent reactivity, polymerization selectivity.

1. Introduction

One specific reaction of the polymerization of acetylene on palladium, the cyclotrimerization, is shown to occur only on an ensemble of at least 7 atoms in the case of Pd(111) single crystals [1]. This indicates that this class of reaction is strongly dependent on the structure even for bulk materials. In the gas phase it has been shown that already atomic metal ions reveal a very interesting chemistry with respect to hydrocarbons (see e.g., in the reviews by Schwarz and Schröder [2,3]). As an example Cox and Kaldor and their coworkers have studied palladium and platinum clusters interacting with a series of alkanes and aromatics [4–6]. In the case of CH_4 on Pt_n with up to n = = 24 atoms, activation was realized for the first time on an unsupported metal cluster, and the reaction had a distinct cluster size dependence, with Pt_2 to Pt_5 being most reactive. Charged $Pt_n^{+/-}$ clusters $(n = 1–9)$ react subsequent elimination of molecular hydrogen H_2, to form the final metal carbene complex $Pt_n^{+/-}CH_2$ [7]. The cation cluster reactions were found in general to proceed more than one order of magnitude faster than the anionic clusters. The platinum tetramer anion is unique in this respect, reacting more efficiently than the corresponding cation. Indications for a correlation of reactivity with the availability of low coordination metal atoms was discussed by Trevor et al. [6]. Thus, it was speculated that low coordination metal atoms activate CH_4 more readily than closed packed metal surface atoms [8]. The propensity of small, Pd clusters to activate methane in a similar manner was also confirmed theoretically [9–11]. This indicates that in contrast to bulk materials already very small, free clusters in the nonscalable size regime reveal rich hydrocarbon chemistry. Indeed, we show in this paper that one metal atom may be enough to catalyze the cyclotrimerization reaction of acetylene. Whether the reaction finally occurs not only depends on the type of atom or the support material and their defects, but also on the dynamics of the atom on the support. Furthermore studies on small clusters revealed the possibility for tuning the branching ratio of the polymerization simply by changing cluster size.

2. Experimental

Monodispersed cluster ions, selected from a distribution of cluster sizes obtained by supersonic expan-

sion of a cold (40 K, estimated from the expansion conditions) laser-generated metal plasma, were deposited on various MgO thin films always kept at 90 K. Most of the total deposition energy, being smaller than the binding energies of the investigated Pd clusters [12], is rapidly dissipated via the solid surface [13]. Therefore, under these conditions the clusters soft-land (that is, without fragmentation) on the substrate [13–15]. That clusters indeed maintain their identity upon deposition is also shown experimentally. The carbonyl formation of small deposited Ni_n (n = 1–30) was studied by exposing the deposited clusters to carbon monoxide [16]. Temperature programmed desorption experiments showed that the nuclearity of the formed Ni_n-carbonyls (n = 1–3) is not changed. The absence of, for example, $Ni(CO)_4$ and $Ni_3(CO)_x$ after deposition of Ni_2, directly indicates that fragmentation upon deposition can be excluded under our experimental conditions. Deposition of less than 1% of a monolayer (ML) of Pd clusters (1 ML = $2.2 \cdot 10^{15}$ clusters/cm^2) at a substrate temperature of 90 K assures isolated supported clusters pinned on the defect sites of the support [12,16–19]. The existence of monodispersed Pd_n clusters is proven by the excellent agreement of the measured vibrational frequencies and binding energies of CO on various cluster sizes with theoretical CO values. The support is prepared in situ by epitaxially growing thin MgO(100) films on a Mo(100) surface. These films show bulk-like properties [20]. Small amounts of defects like steps, kinks and F centers are detected by the desorption behavior of small molecules [21]. To obtain identical conditions for the study of the polymerization on different Pd cluster sizes and Pd, Rh, and Ag atoms we first exposed, using a calibrated molecular beam doser, the prepared model catalysts at 90 K to an average of 1 Langmuir (L) acetylene, corresponding to saturation coverage. In a temperature programmed reaction (TPR) catalytically formed benzene (C_6H_6), butadiene (C_4H_6) and butene (C_4H_8) molecules are detected by mass spectrometry and monitored as function of temperature (heating rate 2 K/s) and cluster size. The cluster reactivities were obtained by a single pass heating cycle. The thermal stabilities of the deposited clusters were investigated by Fourier transform infrared (FTIR) spectroscopy for Pd atoms, which are found not to migrate up to around 400 K. Up to this temperature the vibrational frequency of adsorbed CO is not changing [22]. This rather high stability can be explained by the high binding energy (~ 4 eV) of Pd atoms bound to the F centers. For clusters the binding energy is expected to be even higher and therefore migration is unlikely.

3. Results

3.1. The trimerization reaction on single atoms

In contrast to both, Pd(111), where an ensemble of 7 atoms is needed for the reaction to occur and solid Rh surfaces, which are inert, single Pd as well as Rh atoms catalyze the cyclotrimerization reaction in a temperature programmed reaction experiment and form benzene, which is desorbing at 300 and 430 K, respectively (Fig. 1). Furthermore, the reaction is very selective as no other product molecules of the polymerization reaction (e.g., C_4H_6, C_4H_8) are observed. Similar to the bulk, single Ag atoms do hardly produce any benzene (Fig. 1).

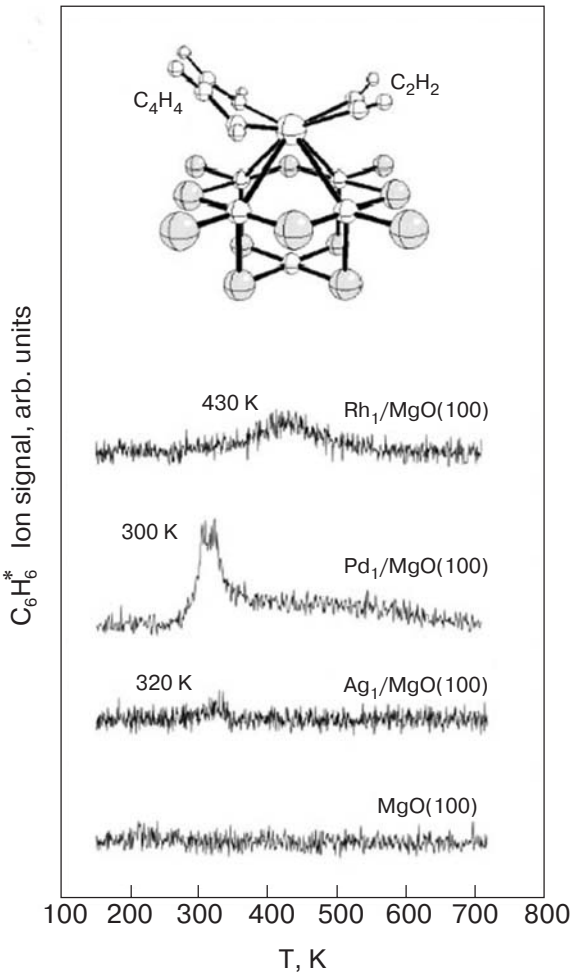

Fig. 1. Temperature programmed reaction spectra of C_6H_6 formed on Ag, Pd, and Rh atoms deposited on defect-rich MgO thin films grown on Mo(100) surfaces. For comparison, the same experiment was performed on a clean defect-rich MgO film. Shown is also the calculated $(C_4H_4)(C_2H_2)/Pd_1/F_{5c}$ intermediate of the cyclotrimerization reaction on Pd atoms adsorbed on an F-center of the MgO(100) surface. For Pd atoms the formation of benzene was also observed at 220 K.

The electronic configurations of the various atoms and their change upon interaction with the support is one key factor for the element specific reactivity. Free Ag atoms do not adsorb C_2H_2 due to the presence of the partially filled 5*s* level. This orbital does not hybridize with the filled 4*d* shell. As it is spatially expanded, it gives rise to a strong Pauli repulsion with the electronic states of the reactant in the entrance channel, thus the reaction is not possible. A free Pd atom ($4d^{10}$) readily adsorbs two C_2H_2 molecules by an average binding energy of 1.35 eV/molecule and transforms them into the C_4H_4 intermediate with an energy gain of 3.9 eV. A third acetylene molecule, however, is only weakly bound and practically not activated. Thus, also a free Pd atom is inert for the cyclotrimerization reaction. With the open *d*-shell configuration, however, Rh atoms become reactive and produce benzene at very low temperature. The first two acetylene molecules adsorb with an energy gain of 1.57 and 1.23 eV, respectively and transform with a very small barrier (0.04 eV) and an energy gain of 0.86 eV into the metallopentacycle, $Rh(C_4H_4)$. The third acetylene molecule is readily adsorbed (0.76 eV) and activated as shown by a change from *sp* to partly sp^2 hybridization. Finally, benzene is formed with a low barrier (0.24 eV) and an energy release of 2.1 eV.

Upon interaction with the MgO support there may be subtle changes in the electronic structure of the atoms, which can result in different reactivities. For Ag atoms, however, these changes are minor and Ag atoms remain inert when adsorbed on the oxide surface (Fig. 1). This is also confirmed theoretically, in fact, activation of Ag atoms would require depopulation of the 5*s* orbital, which is not possible on basic oxides like MgO. Thus the Ag/MgO(F) complex shows no ability to bind acetylene. In contrast to the inert character of Ag atoms, single Pd atoms are turned into an active species when deposited on MgO films and benzene is detected in the thermal desorption spectroscopy (TDS) spectra at 300 K. This astonishing result can be rationalized by studying theoretically the Pd atom adsorbed on different MgO sites. First, a Pd atom on a five-coordinated oxygen ion on the MgO(001) terrace, O_{5c}, is bound by about 1 eV. It was found that the $Pd(C_4H_4)$ complex is indeed formed but the third acetylene molecule is not bound to the complex and therefore this configuration remains catalytically inactive. On four-coordinated steps or three-coordinated corner oxygen sites, O_{4c} and O_{3c}, respectively, the Pd atom binds slightly stronger with an energy of 1.2–1.5 eV, in addition, the atom becomes more reactive. However, on both O_{3c} and O_{4c} sites the third C_2H_2 molecule is only weakly bound or even unbound to the $Pd(C_4H_4)$ surface complex, with the binding energy smaller than the activation energy of the formation of C_6H_6. The interaction of Pd atoms with *F* centers is much stronger, 3.4 eV. On F^+ centers binding energies are with about 2 eV smaller, but still enough toefficiently trap the metal atoms [21]. Furthermore, the presence of trapped electrons at the defect site results in a more efficient activation of the supported Pd atom. In fact, the complex $(C_4H_4)(C_2H_2)/Pd_1/F_{5c}$, Fig. 1, shows a large distortion and a strong interaction of the third C_2H_2 molecule. These results indicate that *F* and F^+ centers can act as basic sites on the MgO surface and turn the inactive Pd atom into an active catalyst. Notice that the supported Pd atoms on defect sites not only activate the cyclization reaction, but also favors benzene desorption, as shown by the very small $(C_6H_6)/Pd_1/F_{5c}$ adsorption energy. The complete reaction path for this specific nanocatalyst has been calculated and is shown in Fig. 2. The first barrier of the reaction path is the one for the formation of the intermediate $Pd(C_4H_4)$ and it is 0.48 eV only. The formation of the C_4H_4 intermediate is thermodynamically favorable by 0.82 eV. On $(C_4H_4)/Pd_1/F_{5c}$ the addition of the third acetylene molecule is exothermic by 1.17 eV, leading to a very stable $(C_4H_4)(C_2H_2)/Pd_1/F_{5c}$ intermediate (Fig. 2). To transform this intermediate into benzene one has to overcome a barrier of 0.98 eV. The corresponding energy gain is very large, 3.99 eV, and mainly related to the aromaticity of the benzene ring. Once formed, C_6H_6 is so weakly bound to the supported Pd atom that it immediately desorbs. Thus, the reaction on Pd/F_{5c} is rate limited in the last step, the conversion of $(C_4H_4)(C_2H_2)$ into C_6H_6. This is different from the Pd(111) surface where the rate determining step for the reaction is benzene desorption. The calcula-

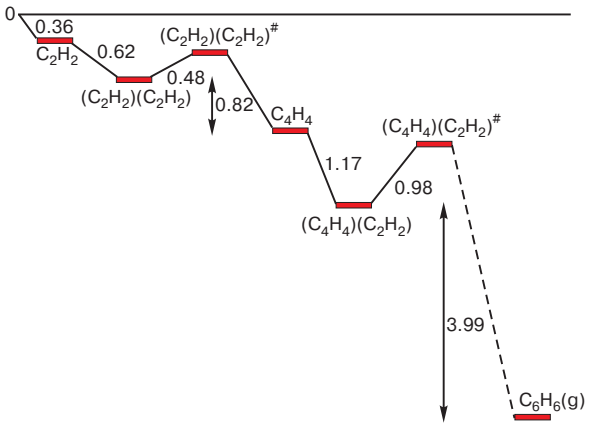

Fig. 2. Computed reaction path for the formation of benzene starting from acetylene promoted by a Pd atom supported on a neutral oxygen vacancy at a MgO terrace, F_{5c} (DFT BP results).

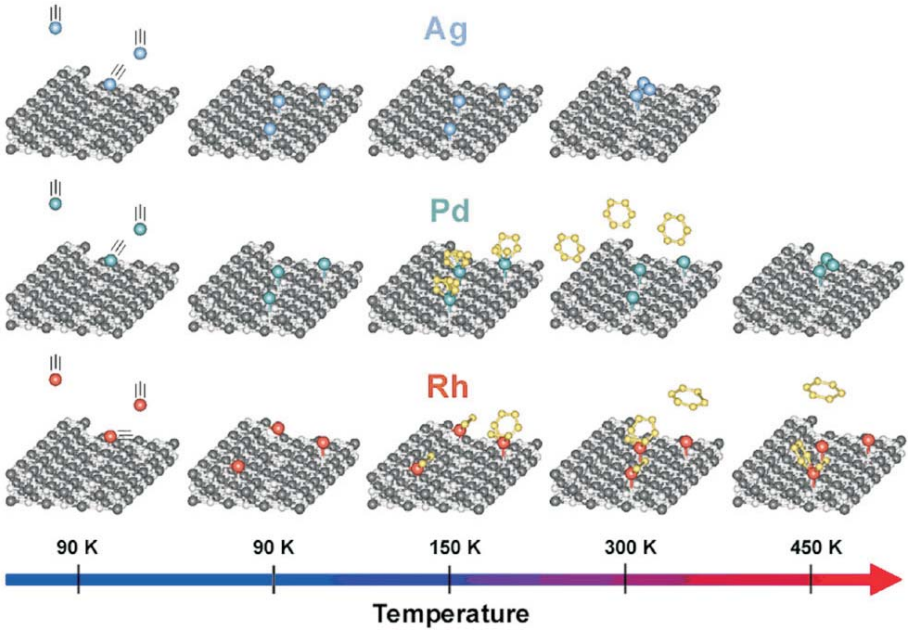

Fig. 3. The proposed mechanisms are shown schematically for the three atoms. Ag and Pd atoms are decorating exclusively *F* centers after deposition whereas Rh is trapped at step edges and *F* centers at 90 K. Ag atoms do not adsorb acetylene and are therefore inert for the reaction. Pd and Rh are forming benzene only when trapped at *F* centers. Note that the relatively broad temperature range for the formation of C_6H_6 on Rh originates from the fact that Rh is trapped at two defect sites at 90 K and that the reaction occurs only after diffusion of the $Rh(C_2H_2)$ complexes from steps to *F* centers. For more details see text.

tions are consistent with the experimental data. In fact, on Pd_1/F_{5c} the computed barrier of 0.98 eV corresponds to a desorption temperature of about 300 K, as experimentally observed (Fig. 1). On Pd (111) surfaces, the bonding of benzene is estimated to be ≈1.9 eV. This binding is consistent with a desorption temperature of 500 K as observed for a low coverage of C_6H_6 on Pd(111) [23]. Thus, this atom is activated on specific sites, *F* centers, on the MgO surface. From FTIR studies and using a the probe molecule, CO, it is known that Pd atoms already diffuse upon deposition to *F* centers and it is this defect site, which activates Pd by a substantial *charge transfer* [24].

A substantial change in reactivity upon deposition is also observed for Rh. In this case, however, Rh atoms are *deactivated*, as the reaction occurs at higher temperature then predicted for the gas-phase by DFT calculations. The product molecule, benzene, is desorbing as a broad peak between 350 and 500 K (Fig. 1). The identification of the involved reaction mechanisms is more complex, as Rh atoms are stabilized at two different trapping centers after deposition and as migration on the MgO surface occurs upon heating (Fig. 3). This indicates that other key factors, the stability and diffusion properties of the deposited atoms, are relevant for the reactivity. In detail, after deposition and prior to acetylene exposure, the majority of the Rh atoms bind to step edges. The calculations show that these Rh atoms strongly interact with a first acetylene molecule by 1.76 eV and the reactant is highly activated as indicated by the long C–C distance (d(C–C) = 1.315 Å), and by the small HCC angle ((H–C–C): 140.2°). The $Rh(C_2H_2)$ complex is strongly bound (2.5 eV) to the surface. The high stability of the $Rh(C_2H_2)$ complex together with steric effects prevent adsorption of a second and third acetylene molecule to form the $Rh(C_2H_2)_2$ and $Rh(C_2H_2)_3$ complexes essential for promoting the reaction. As comparison, for free Rh atoms the two acetylene molecules are bound at opposite sites, a configuration which is not possible when Rh is bound to step edges. Thus, in this configuration Rh atoms do not contribute to the observed formation of benzene. Heating up the model catalysts above room temperature induces migration of the $Rh(C_2H_2)$ complex to those *F* centers, which have not been populated upon deposition of Rh atoms. On *F* centers the $Rh(C_2H_2)$ complex is stably trapped with a binding of 2.8 eV. The computed diffusion barrier for $Rh(C_2H_2)$ from a step (≈1 eV) is considerably lower than the binding energy of acetylene to Rh (1.76 eV), and consequently the whole $Rh(C_2H_2)$ complex is detaching from the step edges and migrates on the surface. Interestingly, when Rh is bound at an *F* center the binding (1.06 eV) and activation (d(C–C) = 1.274 Å;

angle (H–C–C): 149°) of the acetylene molecule is considerably weakened with respect to the step case. This is one of the reasons why Rh can now adsorb a second acetylene molecule from residual reactants in the vacuum chamber by an energy gain of 0.96 eV. At this stage of the process the sample temperature is high enough (> 300 K) that the complex is immediately transformed to the metallopentacycle, $Rh(C_4H_4)$, with a gain of 0.91 eV and overcoming a barrier of 1.18 eV. This complex binds a third acetylene molecule with a binding energy of 1.07 eV and the product is subsequently formed in an exothermic process (3.2 eV). The involved activation energies for the formation of the metallopentacyle ($\Delta E^{\#} = 1.18$ eV) and the formation of benzene ($\Delta E^{\#} = 1.07$ eV) are of the same order but are about 20% higher than for Pd. This explains the higher reaction temperature for Rh. Notice that these are the rate-determining steps as, due to strong Pauli repulsion, benzene desorption requires very little energy (< 0.2 eV) for both, Pd/MgO(F) and Rh/MgO(F). Assuming the Redhead equation with a pre-exponential factor of 10^{13}, the computed barriers correspond to a reaction temperature of about 300 K, which is lower than the temperature of maximal benzene formation at 420 K. In addition, the activation energy for benzene formation is similar to the barrier for detaching the $Rh(C_2H_2)$ complex from step edges. Thus, only Rh atoms initially trapped at *F* centers contribute to the initial formation of benzene at 350 K and the main contribution at higher temperature originates from Rh atoms first trapped at step edges and subsequently turned active after diffusion to the *F* centers. The existence of a distribution of Rh atoms at *F* centers and at step edges prior to reaction therefore explains the rather broad desorption peak of benzene in contrast to the narrow peak observed for Pd, which populates only one kind of defect centers already at the deposition stage. The situation is even more complex as it could be shown that Rh can detach at around 450 K from the *F* centers and form larger clusters [25]. In this context it is important to note that larger Rh_n clusters with $n > 10$ are inert for the cyclotrimerization reaction.

In summary, the specific electronic configuration of Ag renders these atoms inert for the polymerization of acetylene both as free or supported atoms. The reactivity of Pd and Rh is strongly influenced by their adsorption and by their diffusion dynamics on the MgO surface (Fig. 3). Pd atoms are turned into active catalysts for the cyclotrimerization reaction only when adsorbed on *F* centers as charge donation from the defect site to the atom occurs upon bonding. Finally, the low activation barriers of the process on free Rh atoms are substantially increased for Rh adsorbed on a MgO surface and the cyclotrimerization is only catalyzed when trapped on *F* centers as otherwise steric effects, which are especially marked for supported atoms and small clusters, prevent the adsorption of a second or third acetylene molecules on step edges.

3.2. The selectivity of polymerization of acetylene on Pd_n *clusters*

Whereas single Pd atoms are very selective for the formation of benzene, the polymerization of acetylene on larger Pd_n clusters reveal a remarkable pattern in the product formation (Fig. 4). Striking atom-by-atom size-dependent reactivities and selectivities are observed. Only three reaction products C_6H_6, C_4H_8, and C_4H_6 are detected. Interestingly, no C_3H_n, C_5H_n and C_8H_n are formed, indicating the absence of C–C bond scission as already observed on Pd single crystals [26] and Pd particles [27]. Up to Pd_3, only benzene is catalyzed reflecting a high selectivity for the cyclotrimerization of acetylene. Pd_n ($4 \le n \le 6$) clusters reveal a second reaction channel by catalyzing the formation of C_4H_6, too, which desorbs at around 300 K. The third reaction product, C_4H_8, desorbing at a rather low temperature of 200 K, is clearly observed for Pd_8. For this cluster size the abundance of the three reaction products is similar. For even larger clusters ($13 \le n \le 30$) the formation of C_6H_6 is increasing with cluster size, whereas the conversion of acetylene into C_4H_8 reaches a maximum for Pd_{20}. Note that Pd_{30} selectively suppresses the formation of C_4H_6 (the peak in the TPR spectrum of C_4H_6 at 200 K is part of the fragmentation pattern of C_4H_8). For Pd_{20} the experiments were repeated in the presence of D_2 [28]. D_2 was exposed prior and after C_2H_2. The results clearly indicate that no product containing deuterium is formed. Consequently D_2 is not involved in the polymerization reaction. However, the presence of D_2 opens a new reaction channel, the hydrogenation of acetylene. In addition, D_2 blocks the active sites on the palladium clusters for the polymerization, as the formation of the products is slightly reduced when exposing D_2 prior to C_2H_2. On Pd(111), predosing with H_2 completely suppresses the cyclotrimerization but enhances the hydrogenation of acetylene to form ethylene [23].

Assuming stoichiometric reactions, as indicated in Fig. 5, and estimating the relative number of C_2H_2 from Fig. 5,*a* one observes a proportional increase of acetylene with the number of palladium atoms per cluster up to Pd_{13}. Surprisingly, at this cluster size the surface-to-bulk ratio as well as the coordination number of Pd in the cluster is changing as at this size one Pd atom sits completely in the cluster. In addition, according to the free stochiometric chemical reactions, each reaction requires a minimum number of Pd atoms, which are 3, 4, and 6. The experimental results

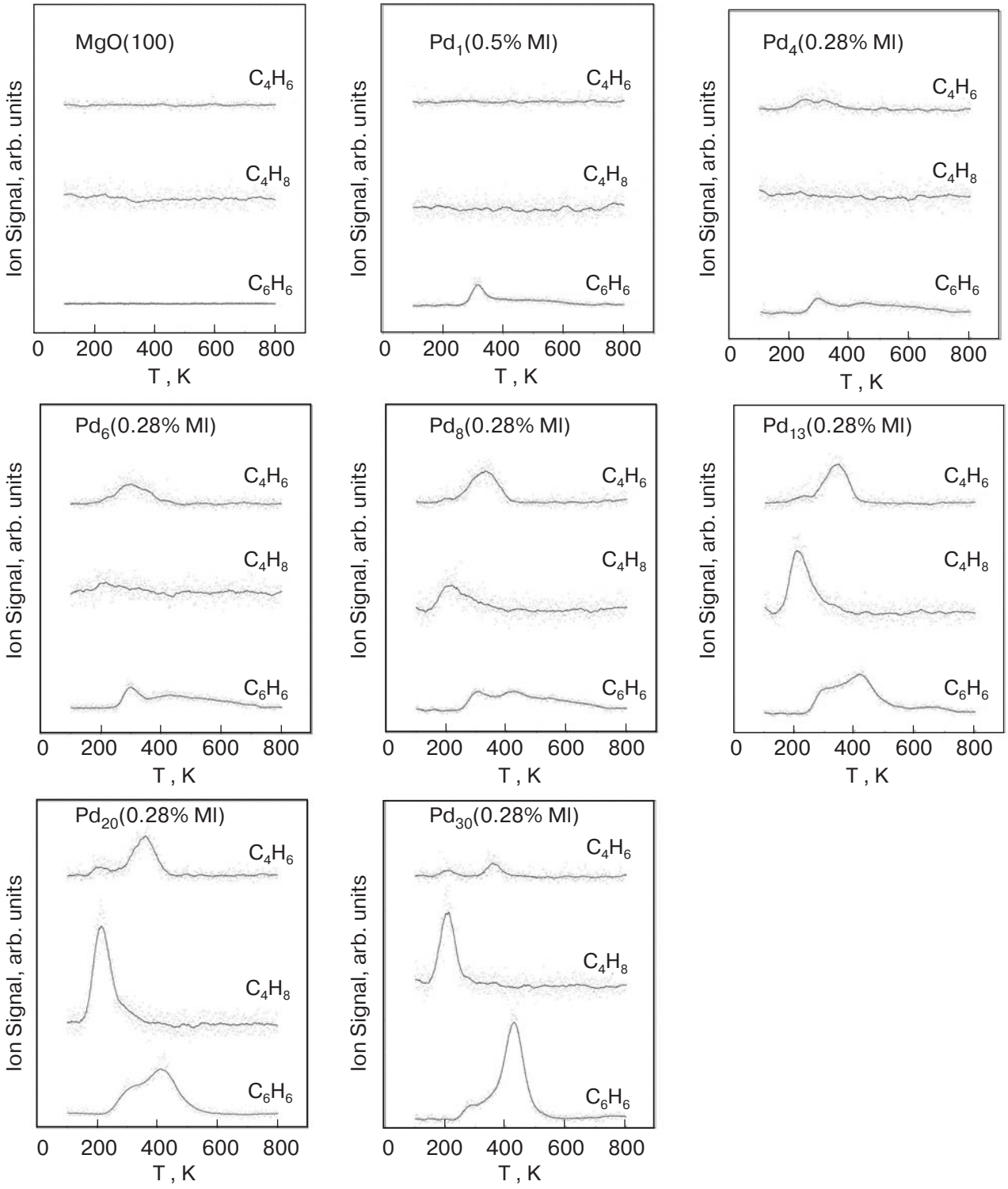

Fig. 4. TPR spectra of the catalytic formation of C_6H_6, C_4H_6, and C_4H_8 for a defect-rich MgO thin film, Pd_1, Pd_4, Pd_6, Pd_8, Pd_{13}, Pd_{20}, and Pd_{30}. The relative ion intensities are corrected with the relative detection efficiencies of the experiment and scale with the number of formed product molecules per cluster.

are surprisingly consistent, that is C_4H_6 is formed for Pd_n with $n \geq 4$ and C_4H_8 for cluster sizes with $n \geq 6$.

Analyzing the products formed on small size-selected Pd_n ($1 \leq n \leq 30$) clusters deposited on MgO(100) thin films indicates that the surface intermediate C_4H_4 is being produced efficiently on all cluster sizes. Thus at least two acetylene molecules are adsorbed in a π-bonded configuration at the initial

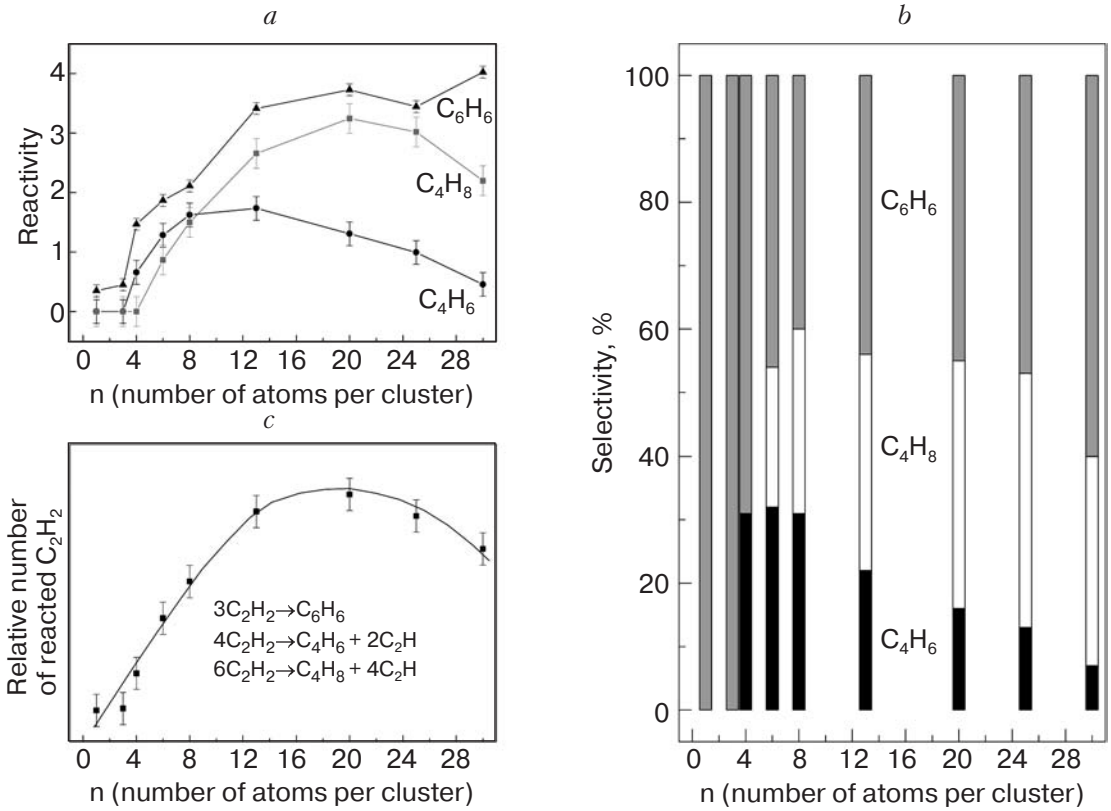

Fig. 5. Reactivity (*a*) (expressed as the number of product molecules per cluster) and selectivity (*b*) (expressed as the relative amount in %) of the polymerization of C_2H_2 on size-selected Pd_n (n = 1–30) deposited on defect-rich MgO thin films. Also shown is the relative number of reacted C_2H_2 as function of cluster size (*c*).

stage of the reaction [12]. The observed size-dependent selectivity may then be understood by regarding the influence of the cluster size to steer the reaction either toward the cyclotrimerization to form C_6H_6 or towards a direct hydrogen transfer from adsorbed C_2H_2 to the C_4H_4 intermediate to catalyze the formation of C_4H_6 or C_4H_8, respectively. Cyclotrimerization is generally observed when a third acetylene molecule is adsorbed in a π-bonded configuration, which results in a change from *sp*-hybridization toward sp^2-hybridization [29]. This bonding configuration leads to a weak activation of the C–H bond, in analogy to ethylene [30]. The hydrogenation of the $Pd_n(C_4H_4)$ metallocycle, on the other hand, is favored by the adsorption of di-σ/π bonded acetylene to three Pd atoms, effecting a more efficient activation of the C–H bond, in analogy to ethylene [30].

As shown above, for Pd atoms adsorbed on defect sites the $Pd(C_4H_4)$ intermediate is readily formed as shown in Fig. 3. A third adsorbed C_2H_2 molecule is purely π-bonded and the activated acetylene molecule reacts with the intermediate to form benzene with a total exothermicity of about 7 eV (Fig. 2). The weakly bound C_6H_6 (0.3 eV) then desorbs at low temperature from the nanocatalyst [12]. A second reaction channel, the formation of butadiene, C_4H_6, opens for Pd_4. This channel reveals highest selectivity for Pd_6, in this case a third C_2H_2 molecule can bind in a di-σ/π bond configuration to three Pd atoms. The charge transfer from the substrate to the cluster further enhances the activation of the C–H bonds. For even larger cluster sizes the adsorption of two di-σ/π-bonded C_2H_2 molecules becomes possible and opens up the third reaction path, the formation of C_4H_8. In our experiments this is clearly observed for Pd_8. Purely geometric arguments (possible adsorption of two di-σ/π-bonded C_2H_2 molecules close to the C_4H_4 intermediate) suggest that this third channel is more pronounced for the larger clusters, and indeed our results show maximal C_4H_8 formation for cluster sizes of 20–25 Pd atoms. For the largest clusters of the measured range, e.g., Pd_{30}, the increased number of metal–metal bonds and the concomitant delocalization of the charge transferred from the substrate to the cluster results in less charge density available for the activation of the C–H bond [31]. Consequently, the cyclotrimerization becomes again more efficient than the hydrogenation of the C_4H_4 intermediate. Going to

even larger particles or to Pd(111) single crystals the cyclotrimerization to benzene is selectively catalyzed.

4. Conclusion

In conclusion, there is no question that a new catalytic chemistry emerges in the non-scalable size regime where every atom counts. This may have important implications for industrial catalysis with respect to low temperature active catalytic materials and selectivity tuning by size-selection. From a more fundamental point of view in particular the combination of gas phase studies, clusters supported on surface, and *ab inito* theoretical simulation are fruitful in defining important nanocatalytic factors and concepts. The most important are the tuning of selectivity and activity by electronic quantum size effects and charging. These factors are unique for small clusters and not observed for bulk catalytic systems or particles in the scalable size regime.

1. R.M. Ormerod and R.M. Lambert, *J. Phys. Chem.* **96**, 8111 (1992).
2. D. Schröder and H. Schwarz, *Angew. Chem. Int. Ed.*, **34**, 1973 (1995).
3. H. Schwarz and D. Schröder, *Pure and Applied Chemistry* **72**, 2319 (2000).
4. P. Fayet, A. Kaldor, and D.M. Cox, *J. Chem. Phys.* **92**, 254 (1990).
5. D.J. Trevor, R.L. Whetten, D.M. Cox, and A. Kaldor, *J. Am. Chem. Soc.* **107**, 518 (1985).
6. D.J. Trevor, D.M. Cox, and A. Kaldor, *J. Am. Chem. Soc.* **112**, 3749 (1990).
7. U. Achatz, C. Berg, S. Joos, B.S. Fox, M.K. Beyer, G. Niedner-Schattenburg, and V.E. Bondybey, *Chem. Phys. Lett.* **320**, 53 (2000).
8. K.J. Klabunde, *Free Atoms, Clusters, and Nanoscale Particles*, Academic Press (1994).
9. M.R.A. Blomberg, P.E.M. Siegahn, and Svensson. *J. Phys. Chem.* **96**, 5783 (1992).
10. Q. Cui, D.G. Musaev, and K.J. Morokuma, *Chem. Phys.* **108**, 8418 (1998).
11. Q. Cui, D.G. Musaev, and K. Morokuma, *J. Phys. Chem.* **A102**, 6373 (1998).
12. S. Abbet, A. Sanchez, U. Heiz, W.-D. Schneider, A.M. Ferrari, G. Pacchioni, and N. Rösch, *J. Am. Chem. Soc.* **122**, 3453 (2000).
13. H.-P. Cheng and U. Landmann, *J. Phys. Chem.* **98**, 3527 (1994).
14. K. Broman, C. Felix, H. Brune, W. Harbich, R. Monot, J. Buttet, and K. Kern, *Science* **274**, 956 (1996).
15. U. Heiz, F. Vanolli, L. Trento, and W.-D. Schneider, *Rev. Sci. Instrum.* **68**, 1986 (1997).
16. U. Heiz, F. Vanolli, A. Sanchez, and W.-D. Schneider, *J. Am. Chem. Soc.* **120**, 9668 (1998).
17. H. Häkkinen, S. Abbet, A. Sanchez, U. Heiz, and U. Landman, *Angew. Chem. Int. Ed.* **42**, 1297 (2003).
18. U. Heiz, A. Sanchez, S. Abbet, and W.-D. Schneider, *J. Am. Chem. Soc.* **121**, 3214 (1999).
19. A. Sanchez, S. Abbet, U. Heiz, W.-D. Schneider, H. Häkkinen, R.N. Barnett, and U. Landman, *J. Phys. Chem.* **A103**, 9573 (1999).
20. M.-H. Schaffner, F. Patthey, W.-D. Schneider, and L.G.M. Pettersson, *Surf. Sci.* **450**, 402 (1998).
21. S. Abbet, E. Riedo, H. Brune, U. Heiz, A.M. Ferrari, L. Giordano, and G. Pacchioni, *J. Am. Chem. Soc.* **123**, 6172 (2001).
22. S. Abbet, A. Sanchez, U. Heiz, W.-D. Schneider, A.M. Ferrari, G. Pacchioni, and N. Rösch, *J. Am. Chem. Soc.* **122**, 3453 (2000).
23. W.T. Tysoe, G.L. Nyberg, and R.M. Lambert, *J. Chem. Soc., Chem. Commun.* **18**, 623 (1983).
24. S. Abbet, A. Sanchez, U. Heiz, W.-D. Schneider, A.M. Ferrari, G. Pacchioni, and N. Rösch, *Surf. Sci.* **454–456**, 984 (2000).
25. K. Judai, S. Abbet, A. Wörz, U. Heiz, L. Giordano, and G.J. Pacchioni, *Phys. Chem.* **B107**, 9377 (2003).
26. C.H. Patterson and R.M. Lambert, *J. Phys. Chem.* **92**, 1266 (1988).
27. R.M. Ormerod and R.M. Lambert, *J. Chem. Soc., Chem. Commun.* **32**, 1421 (1990).
28. S. Abbet, A. Sanchez, U. Heiz, and W.-D. Schneider, *J. Catal.* **198**, 122 (2001).
29. G. Pacchioni and R.M. Lambert, *Surf. Sci.* **304**, 208 (1994).
30. A. Fahmi and R.A. van Santen, *J. Phys. Chem.* **100**, 5676 (1996).
31. S. Burkart, N. Blessing, and G. Ganteför, *Phys. Rev.* **B60**, 15639 (1999).